

Exclusive π^0 electroproduction in the resonance region

Nikolay Markov, Kyungseon Joo,
Maurizio Ungaro, L.C. Smith, Viktor
Moiseev For the CLAS Collaboration

the date of receipt and acceptance should be inserted later

Abstract The exclusive electroproduction process $ep \rightarrow e'p'\pi^0$ was measured in the range of the photon virtualities $Q^2 = 0.4 - 1.0 \text{ GeV}^2$, and the invariant mass range of the $p\pi^0$ system $W = 1.1 - 1.8 \text{ GeV}$. For the first time, these kinematics are covered in exclusive π^0 electroproduction off the proton with the nearly complete angular coverage in the $p\pi^0$ center of mass system with high statistics. Cross section and beam spin asymmetry were measured and structure functions $\sigma_T + \epsilon\sigma_L$, σ_{TT} , σ_{LT} and σ'_{LT} were extracted via fitting the ϕ^* dependence. Analysis of these results revealed the data sensitivity to the contribution from the nucleon resonances $N(1650)1/2^-$, $N(1685)5/2^+$, and $\Delta(1700)3/2^-$. Combined studies of π^+n and π^0p electroproduction off proton data from CLAS at $W > 1.6 \text{ GeV}$ will provide the first results on the high lying N^* and Δ^* electrocouplings at $Q^2 < 1.0 \text{ GeV}^2$ for all excited nucleons with substantial decays to the $N\pi$ final states. These new experimental data will extend the insight into the complex interplay between the inner quark core and outer meson-baryon cloud in the structure of nucleon resonances with masses above 1.6 GeV.

Nikolay Markov
University of Connecticut
E-mail: markov@jlab.org

Kyungseon Joo
University of Connecticut

Maurizio Ungaro
Jefferson Lab

L.C. Smith
University of Virginia

Viktor Moiseev
Jefferson Lab

1 Introduction

The excitation of nucleon resonances via the electromagnetic interaction is an important source of information to understand the structure of excited nucleon states and dynamics of the non-perturbative strong interaction behind resonance formation.

Nucleon resonances with masses less than 1.6 GeV decay preferentially into the $N\pi$ final state and exclusive $N\pi$ electroproduction is the major source of information about the electrocouplings of these states. Many high-lying excited states with masses above 1.6 GeV decay predominantly with the two pion emission [1]. Of the resonances with significant coupling to a single pion channel Δ resonances $\Delta(1700)3/2^-$ and $\Delta(1620)1/2^-$ are better suited to be studied in the single π^0 electroproduction channel due to the selection by isospin Clebsch-Gordan coefficients, although information on N^* states $N(1650)1/2^-$, $N(1675)5/2^-$ and $N(1685)5/2^+$ can also be extracted.

The first excited state of nucleon, $\Delta(1232)$, was extensively studied in the π^0 channel in the wide range of photon virtuality $0 \leq Q^2 \leq 6 \text{ GeV}^2$ [2–8] and magnetic form factor and ratios R_{EM} and R_{SM} of the $N \rightarrow \Delta$ transition extracted. Their values are far from those expected of perturbative regime, $R_{EM} = 1$, and R_{SM} is Q^2 -independent. This suggests that pDQC regime remains far from the achieved values of photon virtualities.

The second resonance region, with its dominant states $N(1440)1/2^+$, $N(1520)3/2^-$ and $N(1535)1/2^+$ is accessible in both π^0 and π^+ channels. Currently, extensive experimental data on these states are available from both reactions. These channels were analyzed within the frameworks of both Unitary Isobar Model (UIM) and dispersion relation (DR) [9] to extract information on the transitional helicity amplitudes $A_{1/2}$, $A_{3/2}$ and $S_{1/2}$ [10]. Based on these results, the successful interpretation of Roper resonance quark core as a first radial excitation of the $3q$ state has emerged and is supported by the light-front relativistic quark models [11,12]. The low- Q^2 behavior of $S_{1/2}$ amplitude of the Roper resonance, while consistent between single and double pion data, show different trends. The single pion data tends to be a constant, while analysis of the $N\pi\pi$ data shows a clear ascending trend as Q^2 goes to zero. Availability of high statistics data at low Q^2 , presented here, will be crucial for resolving this issue.

The characteristic feature of the $D_{13}(1520)$ resonance is a helicity switch from the dominance of the $A_{3/2}$ amplitude at low Q^2 to the dominance of the $A_{1/2}$ at the higher Q^2 . Obtained results are supported by analysis of the $N\pi^+\pi^-$ channel [13]. The CQM prediction for $S_{1/2}$ helicity amplitude of the $S_{11}(1535)$ contradicts the experimental data. CQM expects the amplitude to be positive at $Q^2 \leq 1$, however the data shows that it is clearly negative. This is a strong indication of a significant meson cloud contribution and these data are perfectly suited kinematically to address this problem.

There are recent results [14] on the higher-lying $N(1710)1/2^+$, $N(1675)5/2^-$ and $N(1685)5/2^+$ states obtained in the π^+n channel at high values of photon virtuality $1.8 \leq Q^2 \leq 4.0 \text{ GeV}^2$. While they establish the behavior of resonance

amplitudes at higher Q^2 , lower photon virtualities have not been accessed in the single pion electroproduction.

The single quark transition model (SQTm) [15] approach strongly limits the $A_{1/2}$ and $A_{3/2}$ transition amplitudes of $D_{15}(1675)$ (Moorehouse selection rule, [16]) and while available theories predicts small values of these amplitudes ([17, 18]) experimental data at high Q^2 shows significantly non-zero values for $A_{1/2}$, this opens the possibility to study a meson-baryon cloud effect directly. Data at lower Q^2 will be of great importance as they cover the region between the photon point and $Q^2 < 1\text{GeV}$ and will extend our knowledge of the Q^2 evolution of $A_{1/2}$.

The $A_{3/2}$ amplitude is experimentally found to be around zero at photon virtuality of 1.8 GeV^2 and small but negative at higher Q^2 . The value at the photon point, though, is significantly positive and the presented data covering low Q^2 is expected to show the sharp rise of this amplitude, which serves as a strong indication of the meson-baryon cloud contribution not seen at different kinematics. The predictions of the coupled-channels approach with included meson-baryon contribution [19] predicts a significantly non-zero value of the $A_{3/2}$, but the photon point results remain higher.

2 Experiment and data analysis

The reported experiment was conducted with the CEBAF Large Acceptance Spectrometer (CLAS) in Hall B at Jefferson Lab using a 2.036 GeV electron beam and a liquid hydrogen target. The detector has a nearly 4π angular coverage in the center of mass system, which makes it ideally suited for experiments requiring detection of the several particles in the final state.

To select the exclusive $ep \rightarrow ep\pi^0$ channel, one has to identify events which have electron, proton and π^0 in the final state. To identify electrons, the information of the energy deposited in the calorimeter along with the momentum reconstructed from the curvature of the particle track in the magnetic field is calculated. In this method, electrons can be differentiated from pions due to the fact that their energy deposition in the calorimeter proportional to its momentum, while for the pions it is constant (about 2 MeV/cm).

Proton identification is based on the particle velocity β versus momentum correlation for positively charged particles. β is reconstructed from the TOF information on the track time and DC information of the track length.

Although it is possible to identify a π^0 by detecting two photons in the calorimeter, it would impose unnecessary limitations on the statistics. Instead, one can reconstruct the 4-vector of the missing particle X in the $ep \rightarrow e'p'X$ reaction using the initial and scattered 4-momenta of the electron and proton along with knowledge of the beam energy using momentum conservation.

Overlap of elastic events with single pion events in the missing mass spectrum does not allow for a simple pion separation using a missing mass cut. Instead, careful choice of the suitable cuts allows for the separation of the exclusive single π^0 events from the background. The resulting missing mass distri-

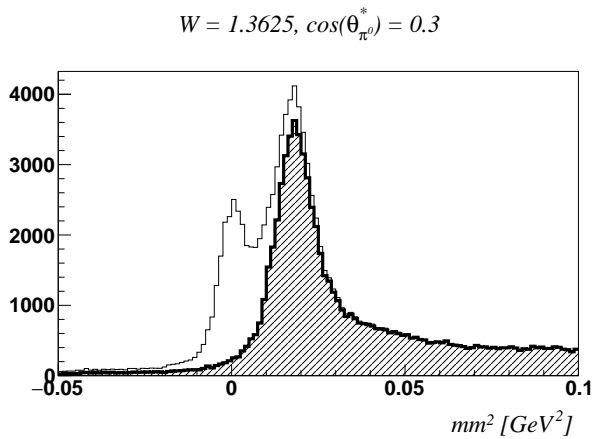


Fig. 1 Bethe-Heitler (BG) event separation. One can not reliably separate BG events from π^0 by means of only missing mass cut, and elaborated procedure, based on the kinematical constraints of the reaction, leads to the selected π^0 event distribution (shaded).

bution is shown in Fig 1. There are two major factors which determine the detector acceptance: geometrical acceptance, which limits the area in which particles could possibly be detected, and detector efficiency. Both are accounted for using a GEANT-based simulation of the CLAS detector called GSIM [21], which includes real detector geometry, materials and magnetic field map. Certain detector inefficiencies, for example non-functioning photomultiplier tubes, are incorporated into data analysis. As an input it receives radiated single π^0 events generated with the *aao.rad* code using MAID07 [22] model. The output of the GSIM program is then reconstructed in the same way as the real experimental data from the detector. Radiative corrections developed in [20] and used in our data analysis, specifically addresses the exclusive pion electroproduction off the proton. It uses a model cross section from MAID07 as an input and calculates the value of the radiative correction, taking in account all four structure functions. In the evaluation of the observables we employed the so called binning correction procedure. The value of the cross section in the center of the given bin does not necessary coincide with the average value of the cross section in that bin. Since MAID07 provides a reasonable description of the cross section shape, it is used to make a correction by 1) dividing bin over four kinematical variables ($W, Q^2, \cos\theta_{\pi^0}^*, \phi_{\pi^0}^*$) into ten smaller bins, 2) calculating average values of the cross section between these 10000 bins (CS_a), 3) calculating the cross section in the center of a large bin (CS_c), and finally 4) taking the ratio of these two numbers.

3 Results

Exclusive π^0 electroproduction cross sections, integrated over the final hadron state angular variables, are presented in Fig 2 as a function of W for the different values of the photon virtuality Q^2 . Three clear resonance-like structures: Δ resonance and bumps located in the second and third resonance regions in the whole Q^2 range accessible in this experiment, is a manifestation of the major feature of the π^0 electroproduction cross section. This opens up a possibility to extract the values of the resonance electrocouplings from the single pion and combined single and double pion channel analysis.

Another manifestation of the significant resonant contribution into the full cross section is presented in Figs. 3 and 4, which show comparisons of the obtained results to the JLAB/YerPhi [23] model prediction and pure resonance contribution to this cross section in the different resonance regions. Resonance electroproduction amplitudes for these calculations are taken from the empirical fit to data on resonance electrocouplings from both single and double pion electroproduction channels.

For the extraction of the nucleon resonance electrocouplings, the results on the exclusive structure functions $\sigma_T + \epsilon\sigma_L(W, Q^2)$, $\sigma_{TT}(W, Q^2)$ and $\sigma_{LT}(W, Q^2)$ are needed. These were obtained by fitting the experimental data on the π^0 CM-angular distributions by the general expression valid for the single photon exchange approximation for the exclusive π^0 electroproduction amplitudes Eq. 1.

In order to express the resonance manifestation in the measured differential cross section $d\sigma/d\Omega_{\pi^0}$, the cross sections were computed within the JLAB/YerPhi model approach with the resonance electrocouplings taken from the fit to the CLAS results [24], available from the studies of $N\pi$, η and $\pi^+\pi^-p$ exclusive electroproduction [25]. Representative examples for the $d\sigma/d\Omega_{\pi^0}$ are shown in Fig. 3, 4.

$$\frac{d\sigma}{d\Omega_{\pi^0}^*} = \frac{2Wp_{\pi^0}^*}{W^2 - m_p^2} (\sigma_T + \epsilon\sigma_L + \epsilon\sigma_{TT} \sin^2\theta_{\pi^0}^* \cos 2\phi_{\pi^0}^* + \sigma_{LT} \sqrt{2\epsilon(\epsilon + 1)} \sin\theta_{\pi^0}^* \cos\phi_{\pi^0}^*) \quad (1)$$

The agreement between the full model calculation and data is good for both plots. One can clearly see that the resonance contribution is significant in the second resonance region and is higher still in the third region. This is a clear indication of the possibility to extract the resonance parameters in the presented data.

Using Legendre decomposition (Eq 2, Eq. 3, Eq. 4) of the structure functions $\sigma_T + \epsilon\sigma_L$, σ_{LT} and σ_{TT} , obtained from the cross section by fitting over ϕ_{π^0} , one can look for the sensitivity of the Legendre polynomial coefficients to the individual resonance. The A_2 Legendre coefficient (A_2) was computed within the JLAB/YerPhi model and with the resonance electrocouplings taken from the interpolation of the CLAS results (red solid line in Fig. 5). We have also

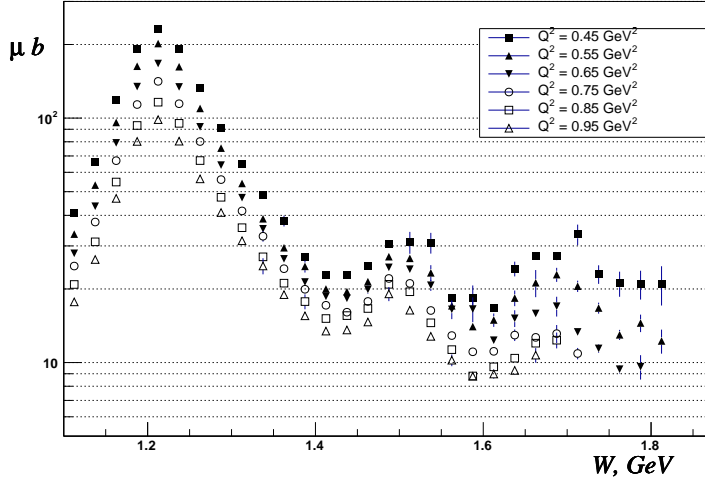


Fig. 2 Fully integrated π^0 electroproduction cross section as a function of W for different values of Q^2 .

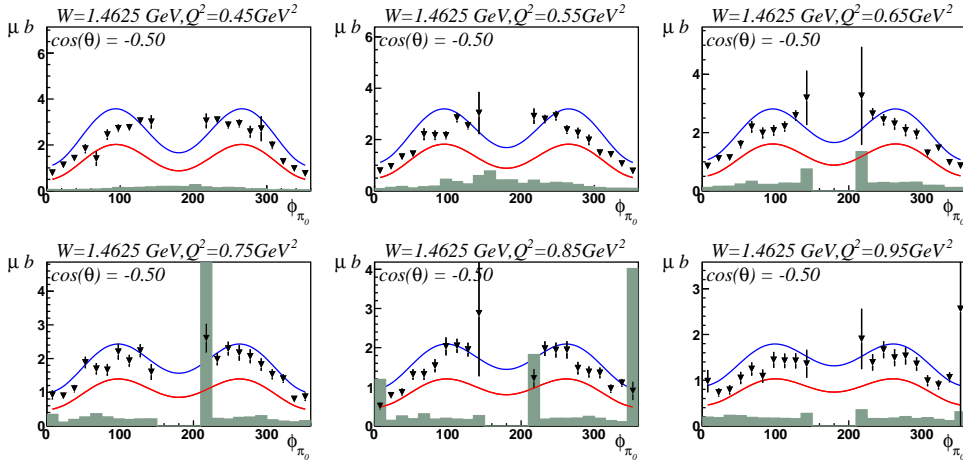


Fig. 3 Differential π^0 electroproduction cross section as a function of ϕ_{π_0} in the CM frame at fixed values of W , Q^2 and $\cos\theta_{\pi_0}$. Blue lines show the full model calculations, red lines show resonance contribution.

computed the same A_2 Legendre coefficient by switching off $A_{1/2}$ and $S_{1/2}$ electroexcitation amplitudes of the $\Delta(1620)1/2^-$ within the model. The results are presented in Fig. 5 by dotted and dashed lines respectively. Switching on/off $\Delta(1620)1/2^-$ electrocouplings causes A_2 coefficient variation outside of the

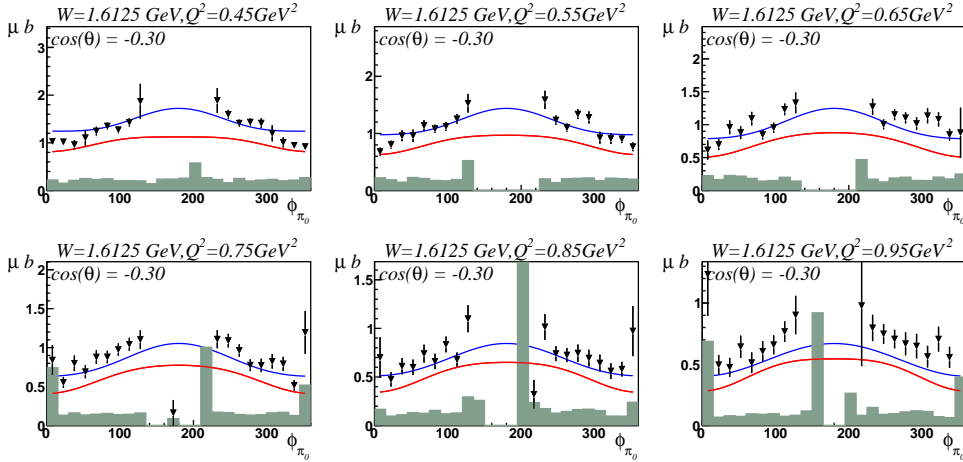


Fig. 4 Differential π^0 electroproduction cross section as a function of the $\phi_{p\pi^0}$ in the CM frame at the fixed values of the W , Q^2 and $\cos\theta_{\pi^0}$. Blue lines how the full model calculations, red line - resonance contribution.

data statistical and systematical uncertainty, suggesting a good opportunity to determine $\Delta(1620)1/2^-$ electrocouplings from our data.

$$\sigma_T + \epsilon\sigma_L = \sum_{i=0}^{2l} A_i P_i(\cos\theta_{\pi^0}^*), \quad (2)$$

$$\sigma_{TT} = \sum_{i=0}^{2l-2} B_i P_i(\cos\theta_{\pi^0}^*) \quad (3)$$

$$\sigma_{LT} = \sum_{i=0}^{2l-1} C_i P_i(\cos\theta_{\pi^0}^*) \quad (4)$$

4 Conclusion

High statistics measurements of the $ep \rightarrow e'p'\pi^0$ process in the W range from 1.1 GeV to 1.8 GeV and photon virtuality range Q^2 in the 0.4 GeV² to 1.0 GeV² with nearly complete angular coverage are presented. For the first time the exclusive π^0 experimental data in these kinematics have become available. Fully differential cross sections are measured with unprecedented accuracy. Unpolarized structure functions $\sigma_T + \epsilon\sigma_L$, σ_{LT} and σ_{TT} are extracted via the $\sin\phi$ fit. Legendre polynomials are fit to the structure functions and show sensitivity of obtained data to the major resonances in full W range.

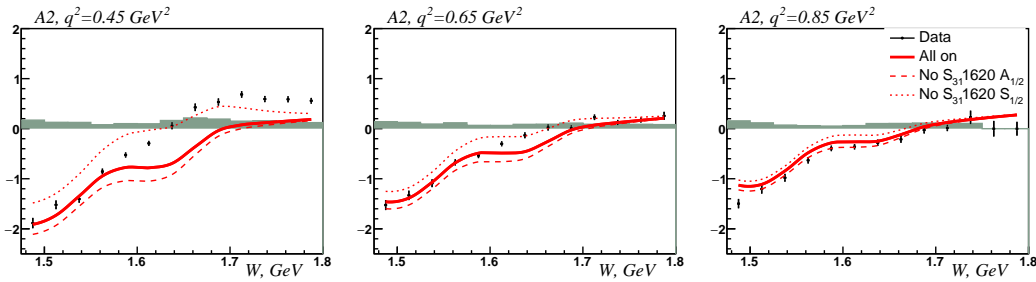


Fig. 5 A_2 Legendre coefficient in the third resonance region as a function of W . The solid lines indicate the full model calculations and the dashed and dotted lines correspond to model calculations with particular helicity amplitudes turned off.

Subsequent analysis of presented the data together with earlier data of this channel, along with information from π^+n production, will provide an opportunity to improve the description of resonant and background mechanisms and reliably obtain the transitional amplitudes of resonance states with mass below 1.8 GeV.

Coupled channel analysis of single and double pion electroproduction channels will further improve our understanding of the mechanisms of the strong interaction in the confinement region. Future extensions of the studies of exclusive meson electroproduction off the proton from the new CLAS data will allow us to explore electrocouplings of the most well established resonances at photon virtualities up to 5 GeV^2 , corresponding to the distance scale where the transition takes place from the combined contribution from meson-baryon cloud and quark core to the N^* structure at small and intermediate Q^2 towards the dominance of quark core only at high Q^2 .

References

1. K.A. Olive et al. (Particle Data Group), *Chin. Phys. C* **38**, 090001 (2014).
2. G. Laveissiere, *Phys. Rev. C* **69**, 045203 (2004).
3. J. J. Kelly, et al., *Phys. Rev. C* **95**, 102001 (2007).
4. J. J. Kelly, et al., *Phys. Rev. C* **75**, 025201 (2007).
5. L.C. Smith et al, Proceedings of the workshop "Shape of hadrons", p.222, Athens, 2006.
6. K. Joo, L. C. Smith, et al., *Phys. Rev. Lett.* **88**, 122001 (2002).
7. M. Ungaro, P. Stoler, I. Aznauryan, V. D. Burkert, K. Joo, L.C. Smith, *Phys.Rev.Lett.* **97**, 112003 (2006).
8. V. V. Frolov et al, *Phys. Rev. Lett.* **82**, 45-48 (1999).
9. I.Aznauryan et al, *Phys.Rev.* **C80**. 055203 (2009).
10. arXiv:1710:02549[nucl-ex].
11. S. Capstick and B. D. Keister, *Phys. Rev. D* **51**, 3598 (1995).
12. I. G. Aznauryan, *Phys. Rev. C* **76**, 025212 (2007).
13. V. Mokeev, *Phys.Rev.* 035203 **C86**. (2012).
14. K.Park, I. Aznauryan, *Phys.Rev.* **C91**, 045203 (2015).
15. I. Aznauryan and V.D. Burkert, *Progr. Part. Nucl. Phys.* **67**, 1, 2012
16. R.G. Moorehouse, *Phys. Rev. Lett.* **16**, 772 1966.
17. M. Ronniger, B. Metsch, *Eur.Phys.J.* **A49**, 8 (2013).

18. E. Satnopinto, M. Giannini, Phys. Rev **C86**, 065202 (2012).
19. B. Julia-Daz, T.-S.H. Lee, A. Matsuyama et al., Phys. Rev. **C 77**, 045205, 12 (2008).
20. A. Afanasev, I. Akushevich, V. Burkert, K. Joo, Phys.Rev. D, **66** 074004 (2002).
21. <https://www.jlab.org/Hall-B/document/gsim/node1.html>
22. D. Drechsel, S.S. Kamalov, L. Tiator, Eur.Phys.J. A **34**, 69-97 (2007).
23. I.G.Aznauryan, Phys.Rev. **C67** (2003) 015209.
24. Nucleon Resonance Photo-/Electrocouplings Determined from Analyses of Experimental Data on Exclusive Meson Electroproduction off Protons, https://userweb.jlab.org/~mokeev/resonance_electrocouplings/
25. Victor I. Mokeev. The 11th International Workshop on the Physics of Excited Nucleons - N*2017, (2017) (See these proceedings).